Resonance properties from a coupled channel meson exchange model*

M. Döring[1;1)] C. Hanhart[1,2] HUANG Fei(黄飞)[3] S. Krewald[1,2] U.-G. Meißner[1,2,4]

1 (Institut für Kernphysik and Jülich Center for Hadron Physics, Forschungszentrum Jülich, D-52425 Jülich,Germany)
2 (Institute for Advanced Simulation, Forschungszentrum Jülich, D-52425 Jülich,Germany)
3 (Department of Physics and Astronomy, University of Georgia, Athens, Georgia 30602, USA)
4 (Helmholtz-Institut für Strahlen- und Kernphysik (Theorie) and Bethe Center for Theoretical Physics, Universität Bonn, Nußallee 14-16, D-53115 Bonn, Germany)

Abstract In this talk, I present the results on the pole structure of pion-nucleon scattering in an analytic model based on meson exchange. The analytic properties of scattering amplitudes provide important information. Besides the cuts, the poles and zeros on the different Riemann sheets determine the global behavior of the amplitude on the physical axis. Pole positions and residues allow for a parameterization of resonances in a well-defined way, free of assumptions for the background and energy dependence of the resonance part. This is a necessary condition to relate resonance contributions in different reactions.

Key words pion-nucleon scattering, meson exchange model, analytic structure of the scattering amplitude

PACS 14.20.Gk, 13.75.Gx, 11.80.Gw

1 Introduction

The global properties of a scattering amplitude are determined by the kinematics of the reaction, leading to branch cuts associated with the opening of reaction channels of stable or unstable particles. The thresholds of two particles or quasi-two particles being on-shell are characterized by the branch points. There is a right-hand and a left-hand cut associated with s channel and crossed channel processes, and there can be resonances, bound and virtual states. Resonances and virtual states are associated with poles on unphysical sheets. Thus, an analytic continuation along the various branch cuts is mandatory to access the resonance poles.

Models of the K matrix type[1—4]and meson exchange models[5—11] provide unitary amplitudes that have been constructed in the past to access pion-nucleon scattering. In unitarized chiral perturbation theory, resonances are described by the non-perturbative interaction of mesons and baryons without the need to explicitly introduce resonance propagators[12—16].

In the present study, we extend the amplitude of the Jülich model to the various Riemann sheets in the complex plane of the scattering energy $s^{1/2} \equiv z$.

The Jülich model is an analytic coupled channel model based on meson exchange that respects two-body unitarity. This model has been developed over the past few years[7, 8], with its current form, as used in this study, given in Ref. [9]. We point out the main ideas in the following. The coupled channel scattering equation is given by

$$T = V + VGT \ , \tag{1}$$

where indices and sums over intermediate quantum numbers have been suppressed. The VGT term implies an integration of the three-momentum. G is the intermediate meson-baryon propagator of the channels with stable particles πN and ηN, and the channels involving quasi-particles, σN, ρN, and πΔ. The pseudo-potential V iterated in Eq. (1) is con-

Received 7 August 2009

∗ Supported by DFG (Deutsche Forschungsgemeinschaft, Gz: DO 1302/1-1), Helmholtz Association through funds provided to the virtual institute "Spin and Strong QCD" (VH-VI-231), EU-Research Infrastructure Integrating Activity "Study of Strongly Interacting Matter" (Hadron Physics2 (227431)) under the Seventh Framework Program of EU and by the DFG (TR 16), COSY FFE (41445282)(COSY-58)

1) E-mail: m.doering@fz-juelich.de

structed from an effective interaction based on the Lagrangians of Wess and Zumino[17, 18], supplemented by additional terms[8, 9] for including the Δ isobar, the ω, η, a_0 meson, and the σ. All these terms contribute to the non-pole part. The pole part is given by baryonic resonances up to $J=3/2$ that have been included in V as bare s channel propagators. The resonances obtain their width from the rescattering provided by Eq. (1).

While, for the channels with stable particles, the analytic continuation to the complex z plane is straightforward, the effective $\pi\pi$N channels require special attention. It is known[19] that the quasi-two particle singularities induce novel structures in the amplitude, i.e. additional branch points in the complex plane, apart from the right-hand $\pi\pi$N cut along the physical axis which has the branch point at $z=m_N+2m_\pi$. The resulting sheet structure is non-trivial and should be fully taken into account; these additional branch points induce large variations of the amplitude in their surroundings and have a large impact on pole positions and residues.

2 Analytic continuation

For the Jülich model, the various sheets are accessed through contour deformation of the momentum integration. In these proceedings we omit the technical details which can be found in Ref. [11].

Only the main structures of the amplitude are pointed out here. As an example of the analytic structure we consider the self energy

$$\Pi_\sigma(z,k)=\int_0^\infty q^2\mathrm{d}q\,\frac{(v^{\sigma\pi\pi}(q,k))^2}{z-2\sqrt{q^2+m_\pi^2}+\mathrm{i}\epsilon} \tag{2}$$

of the propagator

$$G_\sigma(z,k)=\frac{1}{z-\sqrt{k^2+(m_\sigma^0)^2}-\Pi_\sigma(z,k)} \tag{3}$$

of two stable particles ($\pi\pi,\pi$N,ηN). We have chosen here the σ channel in $\pi\pi$ scattering. In Eqs. (2, 3), $v^{\sigma\pi\pi}$ is the vertex, m_σ^0 is the bare σ mass and k is the c.m. momentum. The analytic structure of Π_σ is shown in Fig. 1 as a function of the complex scattering energy z.

This $\pi\pi$ self energy has one branch point at the two-particle threshold, and one right-hand cut along the real z axis. The two Riemann sheets are analytically connected along this cut.

This structure is well-known and the analytic continuation can be obtained either through contour deformation of the q integration or through adding explicitly the discontinuity along the right-hand cut.

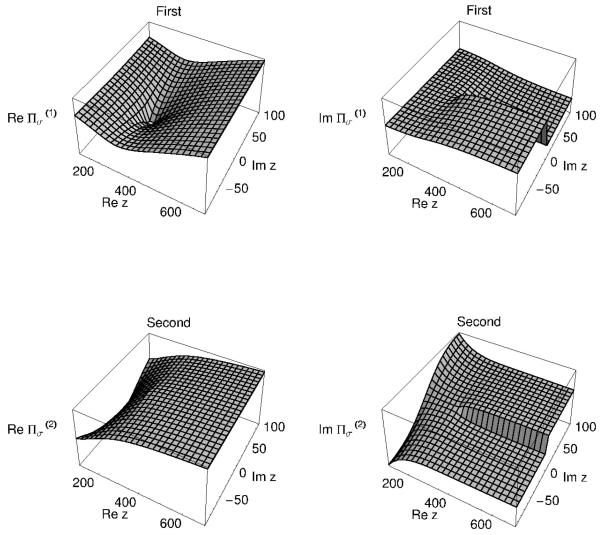

Fig. 1. The two Riemann sheets of the σ self-energy [arb. units] as a function of z [MeV]. The left column shows the real and the right column the imaginary part of Π_σ.

The analytic continuation for the effective $\pi\pi$N channels σN, ρN, and $\pi\Delta$ is different from the channels $\pi\pi$, πN and ηN discussed before. The σN propagator can be parameterized as[9]

$$\begin{aligned}
&g_{\sigma\mathrm{N}}(z,k)=\\
&\frac{1}{z-\sqrt{m_\mathrm{N}^2+k^2}-\sqrt{(m_\sigma^0)^2+k^2}-\Pi_\sigma(z_\sigma(z,k),k)},\\
&G_{\sigma\mathrm{N}}(z)=\int_0^\infty \mathrm{d}k\,k^2\,F(k)\,g_{\sigma\mathrm{N}}(z,k),\\
&z_\sigma(z,k)=z+m_\sigma^0-\sqrt{k^2+(m_\sigma^0)^2}-\sqrt{k^2+m_\mathrm{N}^2}\ ,
\end{aligned} \tag{4}$$

with Π_σ from Eq. (2) and F is a regulator.

It is easy to see that Π_σ induces a right-hand cut in the complex z plane with the corresponding branch point at $z=2m_\pi+m_\mathrm{N}$. Still, there is the quasi-two-particle singularity coming from the denominator in $g_{\sigma\mathrm{N}}$ from Eq. (4). One can show that this singularity is closely connected to the σ pole in $\pi\pi$ scattering. In Ref. [11] it is shown that a new branch point b_2 is induced that is located at

$$z_{b_2}=z_\mathrm{p}+m_\mathrm{N}\ , \tag{5}$$

where $z_\mathrm{p}=875-232\,i$ MeV is the pole position of the σ in the complex z_σ plane. There is another branch point at $z_{b_2'}=z_{b_2}^*$.

Thus, branch points in the complex z plane of the effective $\pi\pi$N propagators are directly related to the pole of the unstable particle. An unstable particle σ induces branch points in the σN propagator.

These branch points are always on the second sheet of $G_{\sigma N}$, as we have seen in the derivation of Eq. (5) in Ref. [11], because this is where the resonance poles are. Furthermore, as there is only one pole on the second sheet of the σ propagator, there are no further induced branch points of $G_{\sigma N}$ in the z plane, apart from b_2 [and b_2' in the upper z half plane].

For the ρN and πΔ propagators, relation (5) holds as well, with the corresponding masses and pole positions; in all cases, the validity has been confirmed numerically.

The resulting analytic structure is shown in Fig. 2.

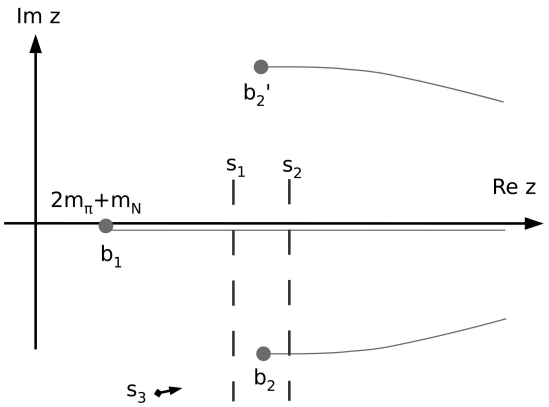

Fig. 2. The full analytic structure of the σN propagator $G_{\sigma N}$. The branch point b_1 is at the ππN threshold and connects first and second sheet. The branch points b_2 and b_2' are located at $z_{b_2} = z_p + m_N$ ($z_{b_2'} = z_p^* + m_N$) and connect second with third, and second with fourth sheet, respectively. The lines s_1 and s_2 indicate slices plotted in Fig. 3.

There is a branch point b_1, located at $z_{b_1} = 2m_\pi + m_N$, which connects first and second sheet[1)], both of them with a cut along the real axis. As we have seen previously, this branch point and its cut are induced by the cut of the σ self-energy Π_σ. The additional branch points b_2 and b_2' lie in the complex plane, both of them on the second sheet, and induce the two additional sheets three and four.

The sheet structure of the σN propagator (only real part) is shown in Fig. 3, along the slices s_1 and s_2 indicated in Fig. 2. The different lines (thick, thin solid, dashed) are obtained following different paths around the branch point b_2. This is explained in detail in Ref. [11]. The dashed lines indicate the presence of a complex conjugate structure, as required by Schwartz's reflection principle.

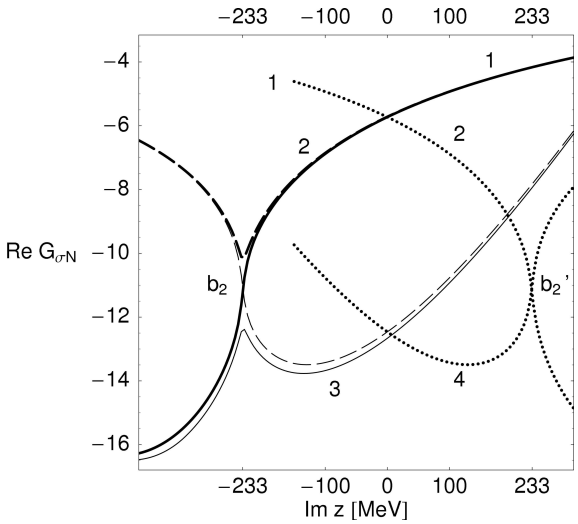

Fig. 3. The analytic structure of all four Riemann sheets [arb. units], labeled 1 to 4, shown close to Re z of the branch points b_2 and b_2'.

The implementation of the analytic continuation in the Jülich model requires some extra work; these technical details are discussed in Ref. [11].

3 Results

In the previous section, the analytic structures of the propagators of channels with stable particles πN, ηN and of effective ππN channels πΔ, ρN, and σN have been determined. The analytic continuations of the propagators determine the analytic continuation of the T matrix. In this section, we determine the properties of $T(z)$ in terms of poles and zeros in the complex z plane.

For a channel with stable particles, there are two sheets, while for unstable particles, there are four as we have seen in the previous section. Thus, for the channel space considered here, there are $2^2 4^3 = 256$ sheets corresponding to the two stable and three effective ππN channels.

Poles of the amplitude are searched for on the second sheet, as defined in Ref. [11]. This second sheet is determined from considerations of connectedness of the sheet to the physical axis; poles on sheets that are not directly connected to the physical axis have little impact on the amplitude. This is discussed in detail in Ref. [11].

The first sheet is free of poles as we have checked. The results for pole positions and residues are summarized in Table 1. The extracted resonance parameters are compared with other studies[20—22], all of them accepted by the PDG[23].

1)The counting of the sheets refers in this section to the one channel case of σN.

Table 1. Resonance parameters in the present study. The z_0 are the pole positions. The moduli $|R|$ and phases θ of the residues correspond to the πN decay channel.

	Re z_0/ MeV	-2Im z_0/ MeV	$\lvert R\rvert$/ MeV	$\theta/(^\circ)$
$N^*(1440)\,P_{11}$	1387	147	48	−64
[20]	1359	162	38	−98
[21]	1385	164	40	
[22]	1375±30	180±40	52±5	−100±35
$N^*(1520)\,D_{13}$	1505	95	32	−18
[20]	1515	113	38	−5
[21]	1510	120	32	−8
[22]	1510±5	114±10	35±2	−12±5
$N^*(1535)\,S_{11}$	1519	129	31	−3
[20]	1502	95	16	−16
[21]	1487			
[22]	1510±50	260±80	120±40	+15±45
$N^*(1650)\,S_{11}$	1669	136	54	−44
[20]	1648	80	14	−69
[21]	1670	163	39	−37
[22]	1640±20	150±30	60±10	−75±25
$N^*(1720)\,P_{13}$	1663	212	14	−82
[20]	1666	355	25	−94
[21]	1686	187	15	
[22]	1680±30	120±40	8±12	−160±30
$\Delta(1232)\,P_{33}$	1218	90	47	−37
[20]	1211	99	52	−47
[21]	1209	100	50	−48
[22]	1210±1	100±2	53±2	−47±1
$\Delta^*(1620)\,S_{31}$	1593	72	12	−108
[20]	1595	135	15	−92
[21]	1608	116	19	−95
[22]	1600±15	120±20	15±2	−110±20
$\Delta^*(1700)\,D_{33}$	1637	236	16	−38
[20]	1632	253	18	−40
[21]	1651	159	10	
[22]	1675±25	220±40	13±3	−20±25
$\Delta^*(1910)\,P_{31}$	1840	221	12	−153
[20]	1771	479	45	+172
[21]	1874	283	38	
[22]	1880±30	200±40	20±4	−90±30

For prominent resonances with large branching to πN, the different analyses are in reasonable agreement with the present results. For other resonances that are wide and/or couple to πN only weakly, the results are much more disperse and there are noticeable differences among the results of Refs. [20—22] and also to the results of the present study. Note that for resonances such as $\Delta^*(1910)$ and $N^*(1720)$, little is known about residues and phases.

A special situation is given for the S_{11} partial wave in which two resonance interfere making the extraction of resonance parameters more difficult. Table 1 shows that the values from the PDB[23] for both $|R|$ and θ are very different in the various studies for the $N^*(1535)$. This is due to the systematic uncertainties from the close-by ηN threshold plus the interference with the $N^*(1650)$. The values of the present study lie within these wide spans. This issue is discussed in detail in Ref. [11] and has been presented on this conference by S. Krewald[24].

3.1 The Roper resonance

The Roper $N^*(1440)P_{11}$ resonance does not require a genuine pole term in the Jülich model[8]. Instead, the resonance shape is dynamically generated from the coupled channel interaction together with the unitarization from Eq. (1). Here, we can confirm this result, because we have indeed found a pole for this resonance.

Yet, there are poles on other sheets which we comment on in the following. Consider a pole that couples only weakly to a given channel, i.e. its residue to e.g. the ρN channel is small. Suppose the pole has been found on the second sheet. Then, at the pole position, the term $(1-VG)^{-1}$ which appears in the solution of Eq. (1) is singular. We consider an element of this matrix and write symbolically, with $G^{(2)}_{\rho N}$ the ρN propagator on the second sheet,

$$(1-VG)=a+bG^{(2)}_{\rho N}=0 \tag{6}$$

omitting further indices, sums and integrations. a contains the terms with intermediate states of other channels. The weak coupling to ρN is reflected by the fact that the b terms are small compared to the a terms, and the replacement $G^{(2)}_{\rho N}\to G^{(3)}_{\rho N}$ does not change much the position of the zero; the resonance pole will reappear on the third or even fourth ρN sheet.

Such replica of poles on other sheets have no physical implications. E.g., in the partial wave analysis SP06 of Ref. [20], a pole of the Roper has been found at $z_0=1359-81\,i$ MeV on the second πΔ sheet (in their counting: first sheet), and another one at $z_0=1388-83\,i$ MeV on the third πΔ sheet (their counting: second). Also in the present study, we find a second pole of the Roper on the third πΔ sheet at $z_0=1387-71\,i$ MeV which is just a few MeV away from the pole on the second sheet quoted in Table 1.

As discussed before, this is rather a replica of the pole on the second sheet, without physical implications, than a genuinely new structure; indeed, within the Jülich model the coupling strength of the Roper to the πΔ channel is moderate; a change of sheets

does not change much the resonance properties in this special case.

The rather different pole positions and residues of the two Roper poles in Ref. [20] indicate a larger coupling to the $\pi\Delta$ channel, and in this case the branch point b_2 plays an important role as stressed in Ref. [20] which makes a simple Breit-Wigner parameterization of the Roper questionable[20]. In the Jülich model, the $\pi\pi$N inelasticity of the Roper is rather given by the effective σN channel[8].

The σN channel has its quasi-two-body singularity at much higher energies than the nominal position of the Roper. Indeed, it is not the pole of the σ which is important at the energies of the Roper, but the $\pi\pi$-correlation in the σ channel, that opens at $z = m_{\rm N} + 2m_\pi$. This correlation is taken into account through a fit to the $\pi\pi$ phase shifts, with the result shown in Ref. [7], Fig. 10. There are residual discrepancies, but those cannot change qualitatively the result.

It still remains to be seen whether the strong σN channel, as found in the Jülich model, can deliver a consistent pictures in other reactions such as pion electroproduction.

In Table 2, we compare the positions of the various zeros of the present study (second sheet) with the results from Ref. [25]. The results agree qualitatively.

Table 2. Position of zeros of the full amplitude T in (MeV).

first sheet		second sheet		Ref. [25]
P_{11}	$1235-0\,i$	S_{11}	$1587-45\,i$	$1578-38\,i$
D_{33}	$1396-78\,i$	S_{31}	$1585-17\,i$	$1580-36\,i$
		P_{31}	$1848-83\,i$	$1826-197\,i$
		P_{13}	$1607-38\,i$	$1585-51\,i$
		P_{33}	$1702-64\,i$	–
		D_{13}	$1702-64\,i$	$1759-64\,i$

3.2 A pole on the third ρN sheet

The analytic properties of an amplitude with unstable particles can imply complex structures one of which is discussed in the following. In Fig. 4, the D_{13} partial wave is shown. The full solution is indicated with the red solid lines and reproduces well the partial wave analysis from Ref. [26].

The blue dotted lines represent the non-pole part $T^{\rm NP}$ as defined in Ref. [10], i.e. the amplitude without the s-channel resonance exchange diagrams. The pole term $T^{\rm P}$ contains the s channel exchanges and the full amplitude is given by $T = T^{\rm NP} + T^{\rm P}$[10].

A resonant structure in $T^{\rm NP}$ is visible at around $z \sim 1.7$ GeV, which disappears in the full solution $T = T^{\rm NP} + T^{\rm P}$. The second Riemann sheet of $T^{\rm NP}$, however, is free of poles. Instead, the cut structure from the ρN branch point b_2 at $z_{b_2} = 1702 - 64\,i$ MeV from Fig. 2 is enhanced. This is a sign that there is structure on the third ρN sheet. This is indeed the case. Using the prescriptions from Ref. [11], it is possible to analytically continue the amplitude of the Jülich model to the third ρN sheet. Indeed, there is a pole at 1613—$83\,i$ MeV. It has a strong coupling to the ρN channel and a medium size coupling to πN and is, thus, a state dynamically generated mainly from the attractive interaction in the ρN channel. Recently, a dynamically generated pole at a similar energy and also with a strong ρN S-wave coupling has been found in Ref. [27].

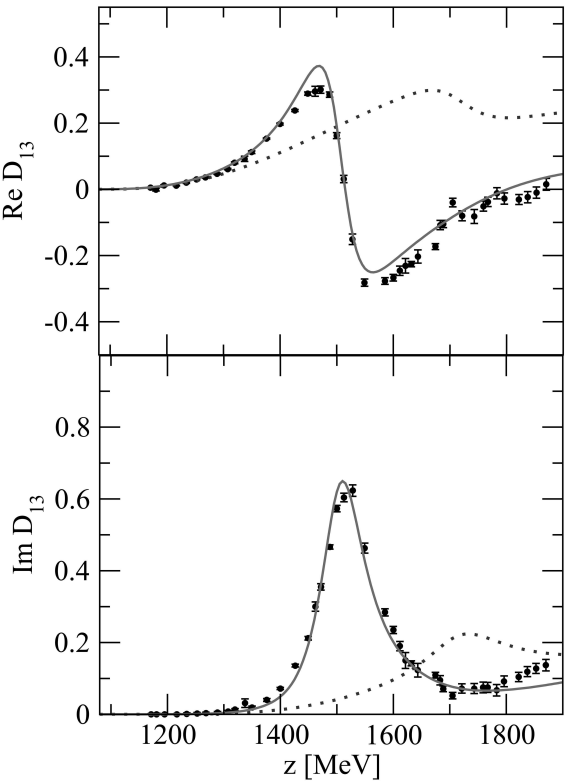

Fig. 4. Amplitude in the D_{13} partial wave.

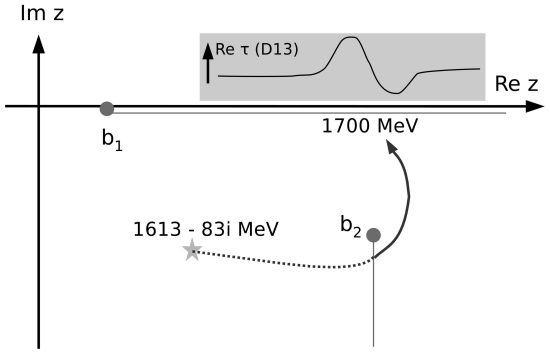

Fig. 5. The D_{13} pole in $T^{\rm NP}$ on the third ρN sheet and its influence at the physical axis. The insert shows schematically the structure visible in $T^{\rm NP}$.

Figure 5 illustrates the effects of a pole on the third sheet: A path from the pole position to the physical axis must necessarily pass around the branch point b_2 to get from the third sheet to the second sheet that connects to the physical axis. The part of the path on the third sheet is indicated with the dotted lines in Fig. 5. The straight red line indicates our choice of the cut, where second and third sheet are connected [cf. Ref. [11]]. Once on the second sheet (solid blue line), it is possible to approach the physical axis on a straight path.

In other words, the pole on the third sheet can affect the physical amplitude only via a detour around b_2. The structure in the physical amplitude is, thus, rather located at the position of b_2 than at the actual pole position.

Summarizing, the branch points b_2 of effective $\pi\pi$N channels lead to complex structures of the amplitude. The structure that appears as a resonance on the physical axis is fact a threshold effect of the quasi-two-particle threshold ρN associated with b_2; it is induced by a pole at a different position, on a sheet that is not directly accessible from the physical axis.

The situation of the two-pole structure of the Roper discussed in the previous section is similar: there is a Roper pole on the physical $\pi\Delta$ sheet, and a pole on the hidden, third, $\pi\Delta$ sheet; the pole on the hidden sheet, wherever it is, can never be seen directly but will appear as a washed out cusp from the quasi-two-body singularity, always in superposition with the contribution from the pole on the physical sheet.

The pole part $T^{\rm P}$ in D_{13} is given by the N*(1520) resonance, introduced as a genuine resonance state. Once $T^{\rm P}$ is summed to $T^{\rm NP}$, the full solution $T = T^{\rm P} + T^{\rm NP}$ is obtained, indicated with the solid lines in Fig. 4. The dynamically generated structure in $T^{\rm NP}$ has then disappeared due to the mechanism of resonance repulsion discussed in Ref. [10] and also presented on this conference[24] for the case of the $\Delta(1232)$.

4 Summary

The analytic structure of the Jülich model has been determined. There are two sheets for every channel of stable particles and four sheets for every effective $\pi\pi$N channel. Poles and residues have been determined.

The amplitudes of the Jülich model are derived within a field theoretical approach from Lagrangians obeying chiral constraints. Data are described to a high precision in the various partial waves. We claim that with these ingredients, in combination with a thorough treatment of the analytic properties, a reliable and precise extraction of pole positions and residues becomes possible.

References

1 Anisovich A V et al. Eur. Phys. J. A, 2005, **25**: 427
2 Manley D M et al. Phys. Rev. D, 1992, **45**: 4002
3 Penner G et al. Phys. Rev. C, 2002, **66**: 055211
4 Shklyar V et al. Phys. Rev. C, 2005, **71**: 055206, [Erratum-ibid. C, 2005, **72**, 019903]
5 Sato T et al. Phys. Rev. C, 1996, **54**: 2660
6 Julia-Diaz B et al. Phys. Rev. C, 2007, **76**: 065201
7 Schutz C et al. Phys. Rev. C, 1998, **57**: 1464
8 Krehl O et al. Phys. Rev. C, 2000, **62**: 025207
9 Gasparyan et al. Phys. Rev. C, 2003, **68**: 045207
10 Döring M at al. arXiv: 0903.1781 [nucl-th]
11 Döring M at al. arXiv: 0903.4337 [nucl-th]
12 Kaiser N et al. Phys. Lett. B, 1995, **362**: 23
13 Oller J A et al. Nucl. Phys. A, 1997, **620**: 438, [Erratum-ibid. A **652** (1999) 407]
14 Jido D et al. Nucl. Phys. A, 2003, **725**: 181
15 Kolomeitsev E E at al. Phys. Lett. B, 2004, **585**: 243
16 Döring M et al. Phys. Rev. C, 2006, **73**: 045209
17 Wess J et al. Phys. Rev., 1967, **163**: 1727
18 Meißner U G. Phys. Rept., 1988, **161**: 213
19 Frazier W R et al. Phys. Rev., 1964, **134**: B1307
20 Arndt R A et al. Phys. Rev. C, 2006, **74**: 045205
21 Höhler G. πN Newsletter, 1993, **9**: 1
22 Cutkowsky R E et al. Phys. Rev. D, 1979, **20**: 2839
23 Amsler C et al (Particle Data Group). Phys. Lett. B, 2008, **667**: 1
24 Krewald S. Talk at the Workshop on the Physics of Excited Nucleon—NSTAR2009, Beijing April 19—22, 2009.
25 Arndt R A et al. Phys. Rev. C, 2004, **69**: 035213
26 Arndt R A et al. Eur. Phys. J. A, 2008, **35**, 311
27 Oset E et al. arXiv: 0905.0973 [hep-ph]